ESCUELA TÉCNICA SUPERIOR DE INGENIERÍA
INDUSTRIAL DE BARCELONA

UNIVERSIDAD POLITÉCNICA DE CATALUÑA

"Synthesis, characterization and biomedical applications of microbial polymalic and polyglutamic acids derivatives."

Presentado por: José Antonio Portilla Arias

Trabajo realizado bajo la dirección de los Drs.
Sebastián Muñoz Guerra y Montserrat García Álvarez

Barcelona, Febrero 2008

Biodegradable nanoparticles of partially methylated fungal poly(β,L-malic acid) as a novel protein delivery carrier

Summary

The preparation of nanoparticles from 75% methylated poly(β,L-malic acid) was described. The degradability of these particles in aqueous environment was examined and the influence of pH and lipase on hydrolysis rate was evaluated. A set of six proteins differing in molecular weight and/or isoelectric points were used to estimate the loading efficiency of the nanoparticles. Encapsulation, physical absorption and surface chemical grafting were the methods explored for protein entrapping. The amount of protein retained in the nanoparticles was found to be mainly determined by the acid/basic character of the protein and best results were achieved when encapsulation was the method of choice. Protein release from the loaded nanoparticles upon incubation in water under physiological conditions encompassed polymer hydrolysis and happened steadily within periods of times ranging between 3 and 10 days. A preliminary evaluation of the activity loss of entrapped α-chymotrypsin caused by loading and releasing indicated a lower effect in the case of encapsulation. In this case, the enzymatic activity was better sustained even than for the free protein suggesting a beneficial effect of this carrier system on protein preservation.

8.1. Introduction

Nanoparticles are well known to be excellent systems for the adequate biological distribution of drugs, proteins or DNA, both at the cellular and organ levels. The nanometer-size ranges of these delivery systems offer distinct advantages as effective permeation through cell membranes and good stability in the blood flow. However, there are still some problems that should not be ignored, such as the difficulty to control degradation rate and drug release, and nanoparticle stability in salted media, among others. Several biodegradable polyesters such as poly(lactic acid), poly(glycolic acid), polycaprolactone and their copolymers have been used for preparing nano-sized particles for multiple drug delivery applications. The degradation rate and therefore the drug release rate in these particles can be controlled by adjusting the molecular mass of the polymers and additionally, the composition and microstructure in the case of copolymers.[1-3]

The manufacture of polymer particles for protein delivery carrier systems requires special precautions because the complex structure of the protein molecule and its sensitivity to undergo conformational changes. Protein aggregation or/and denaturation caused by either strong interactions with the polymer matrix or solvent effects during entrapping should be minimized without severe loss in the loading capacity. Thus, high loading efficiency and protein activity retention continue to be major challenges in the development of such systems. A large amount of published work reports on the successful preparation of nano and microparticles made of poly(D,L-lactic-*co*-glycolic acid) (PLGA) containing pharmaceutical proteins.[4,5]

Nevertheless, Griebenow *et al.*[6,7] have shown that severe perturbations in the secondary structure of γ-chymotrypsin took place when this protein was encapsulated in PLGA using the solid-in-oil-in-water technique.

Poly(malic acid) (PMLA) is a carboxylic-functionalized polyester that can be produced by both chemical synthesis and by cultivation of fungi.[8] PMLA is perfectly biodegradable and biocompatible and it is metabolized in the mammalian tricarboxylic acid cycle.[9] Some PMLA derivatives are already used as components of crosslinked prodrugs, scaffolds for tissue regeneration[10], and more recently, as a nanoconjugate prototype of drug delivery system for brain cancer chemotherapy.[11,12] Coupling of PMLA with cationic surfactants bearing long linear alkyl chains produces stable ionic complexes able to lodge hydrophobic drugs in the paraffinic subphase.[13,14]

PMLA is readily water-soluble and it is hydrolyzed very fast in aqueous environment. The hydrolysis rapidly proceeds yielding malic acid as final degradation product. Blocking of carboxylic side groups of PMLA decreases the hydrolysis rate and its solubility in water. Recently we have reported on the hydrodegradation of methyl esters of fungal PMLA for a wide range of esterification degrees. Microparticles prepared from fully methylated PMLA were found to release erythromycin in aqueous environment by a mechanism that is largely influenced by the hydrolysis taking place in the host polymer.[15]

In the present work we investigate the copolyester coPMLA-(Me$_{75}$H$_{25}$), (Scheme I) which is a PMLA with 75% of the carboxylic groups modified as methyl esters, regarding nanoparticle preparation and protein loading and releasing. The chemical structure of this copolyester is shown below. This compound is non water soluble but continues displaying a remarkable hydrophilicity and is still readily degradable.

A set of proteins differing in molecular weight or/and isoelectric point were used as models for this study. We explore the formation of nanoparticles in different solvents and characterize some of their physicochemical properties, such as particle size, zeta potential and loading capability. Finally, protein release from the loaded particles and protein activity retention are examined in order to evaluate the potential of this system as a novel protein delivery carrier.

coPMLA-(Me$_{75}$H$_{25}$)
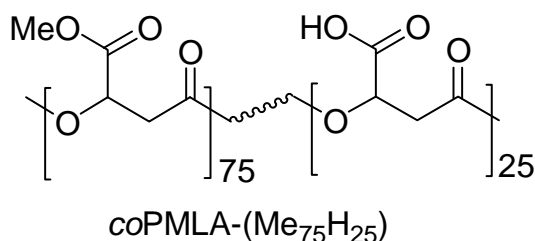
Scheme I. Chemical Structure of copolymer studied in this work.

8.2. Experimental

8.2.1. Materials. Poly(β,L-malic acid) (PMLA) used in this work was obtained by cultivation of *Physarum polycephalum* and purified as described in detail elsewhere.[16] The polyacid was NMR pure and it had a $M_w = 34,300$ Da and $M_w/M_n = 1.08$.

Lipase from *Candida cylindracea* (1,310 units·mg^{-1}), bovine serum albumin (BSA), bovine milk β-lactoglobulin (Lg), myoglobin (Myo) from horse heart and cytochrome-c (Cyt) from bovine heart, were purchased from Sigma. α-Chymotrypsin (Chy) from bovine pancreas (55 units·mg^{-1}) and lysozyme (Lys) from hen egg white were purchased from Fluka. Water soluble *N,N'*-diisopropylcarbodiimide (WSC) was purchased from Aldrich. All organic solvents were analytical grade and used without further purification. Water used for buffers preparation was distilled and deionized in a "Milli-Q" system.

8.2.2. Esterification. The partial esterification of PMLA was performed as described recently elsewhere.[15] In brief, a solution of diazomethane in ether (12.5 mequiv) was added to a solution of PMLA in dry acetone (4.3 mequiv) and the mixture left under stirring at room temperature for 1 h. The reaction mixture was then evaporated under vacuum and the residue dissolved in a small amount of NMP and precipitated in cold diethyl ether. *co*PMLA-(Me$_{75}$H$_{25}$) was recovered by filtration as a white powder in 97% yield. The main features of this copolyester in connection with the present work are given in Table 1.

Table 1. Data of *co*PMLA-(Me$_{75}$H$_{25}$)

[a]Methylation (%)		75.1
[b]Mw/Mn		34,200/26,700
[c]T$_g$/T$_m$ (ºC)		45/171
[d]T$_d$ (ºC)		202
[e]Microstructure		
	n_{Me}	17.4
	n_{COOH}	4.8
	R	0.3

[a]Copolymer composition determined by ^{1}HNMR. [b]Weight and number average molecular weight measured by GPC. [c]Glass transition (T$_g$) and melting (T$_m$) temperatures measured by DSC. [d]Onset decomposition temperature measured at 5% of loss of initial weight. [e]Length of methyl malate (n_{Me}) and malic acid (n_{COOH}) sequences, and randomness (R) determined by ^{13}CNMR analysis.

8.2.3. Nanoparticles: preparation and degradation. Nanoparticles of *co*PMLA-(Me$_{75}$H$_{25}$) were prepared by the precipitation-dialysis method. 10 mg of the copolymer were dissolved in 1 mL of the organic solvent of choice (DMSO, NMP or DMF) and the same volume of water added to yield a translucent solution. The particles were generated upon dialysis of the solution against distilled water for 72 h at room temperature using cellulose membrane tubes (8,000 molecular weight cut-off).

Distilled water was replaced at 2, 24 and 36 h of treatment and the final dialyzed solution was freeze-dried.For hydrolytic degradation studies, aliquots of *co*PMLA-(Me$_{75}$H$_{25}$) nanoparticles were dispersed in buffered saline solutions of different pH's (4.0 citrate buffer, 11.0 Na$_2$HPO$_4$/NaOH buffer, and 7.4 phosphate saline buffer) and incubated at 37 ºC. The enzymatic degradation study was carried out using lipase in phosphate buffered saline (PBS) solution of pH 7.4 at 37°C at a concentration of 0.1 mg·mL^{-1}. In all cases, aliquots were withdrawn at predetermined time intervals, and variations in molecular weight of the degraded nanoparticles were measured by gel permeation chromatography.

8.2.4. Protein loading

Method I*: Encapsulation.* To prepare the protein-encapsulated nanoparticles, 1–8 mg of protein dissolved in 1 mL of PBS, pH 7.4, and 10 mg of *co*PMLA-(Me$_{75}$H$_{25}$) dissolved in 1 mL of DMSO were mixed and the precipitated nanoparticles were collected by centrifugation. To remove the protein physically absorbed onto the surface, the nanoparticles were repeatedly rinsed with water and buffer saline solution of pH higher than the isoelectric point of the protein.

Method II*: Physical absorption.* 10 mg of freeze-dried nanoparticles were added to a solution of 1-8 mg of protein in 10 mL of PBS, pH 7.4 and incubated at 4 ºC for 24 h.

Method III*: Chemical immobilization.* In order to activate the carboxyl groups of *co*PMLA-(Me$_{75}$H$_{25}$) nanoparticles, 10 mg of freeze-dried nanoparticles were suspended in 10 mL of PBS, pH 5.8 and the suspension left to react with 0–1500 μg/mL of WSC for 20 min. The activated nanoparticles were collected by centrifugation and added to a solution of 10 mg·mL^{-1} of protein in PBS, pH 7.4 and the mixture left at 4 ºC for 24 h. After incubation, the nanoparticles were separated by centrifugation and washed as described above.

To evaluate the loading efficiency, protein-encapsulated and protein-adsorbed nanoparticles (10 mg) were dissolved in 5 mL of 4% aqueous sodium dodecyl sulfate (SDS) and the amount of protein present in the solution was determined by the Lowry method.[17] In the case of protein-immobilized nanoparticles, the unreacted protein remaining in the activation reaction mixture was quantified by the Lowry method and the amount of covalently bonded protein determined by difference with the initial amount of protein added.

8.2.5. In vitro release studies and protein activity measurements. Microspheres loaded with proteins (encapsulated, adsorbed and immobilized) (40 mg) were placed in 2 mL of PBS, pH 7.4 and incubated at 37 °C. At scheduled times the nanoparticles were filtered off and the concentration of released protein determined by measuring the absorbance at 280 nm. These values were used to construct the cumulative release profiles. All release experiments were performed by triplicate.

The enzymatic activity of entrapped α-chymotrypsin was determined using of benzoyl L-tyrosine ethyl ester (BTEE) as a substrate. The assay was performed as follows: 0.2 mL of the released α-chymotrypsin solution was diluted with 1.8 mL of buffer (0.05 M Tris-HCl, pH 8.0) and added with 0.2 mL of methanol solution of BTEE (0.3 mg·mL^{-1}). The mixture was placed in a quartz cell and the absorbance changes taking place with time were followed in a UV-spectrometer. The specific activity of the released α-chymotrypsin was calculated taking as reference the activity of the free enzyme measured under the same conditions.

8.2.6. Measurements. Gel permeation chromatography (GPC) was performed using a Waters equipment provided with a refractive index detector and using 0.005M sodium trifluoroacetate-hexafluoroisopropanol (NaTFA-HFIP). Chromatograms were calibrated against PMMA standards.

Scanning electron microscopy (SEM) was used to examine the surface morphology of the nanoparticles before and after degradation. Gold coating was accomplished by using a Balzers SDC-004 Sputter Coater. The SEM micrographs were taken with a JEOL SSM-6400 instrument.

Particle size distribution and zeta potential of nanoparticles in aqueous solution were measured by triplicate by Non-Invasive-Back-Scatter (NIBS) and electrophoresis M3-PALS techniques respectively in a Zetasizer Nano ZS, Malvern.

8.3. Results and discussion

8.3.1. Preparation and characterization of coPMLA-(Me$_{75}$H$_{25}$) nanoparticles. The nanoparticles used in this study have been prepared applying the well established precipitation-dialysis method. It is well known that the solvent used to dissolve the polymer exerts a significant influence on the morphology and physicochemical properties of the nanoparticles.

The copolymer *co*PMLA-(Me$_{75}$H$_{25}$) is readily soluble in several water-miscible organic solvents such as DMSO, DMF and NMP. These solvents have been essayed in this study and the particle size distribution profiles obtained in the three cases are compared in Figure 1a. Although the average size of the nanoparticles did not differ significantly from one solvent to other, a much sharper distribution was found when DMSO was the solvent of choice.

These particles are essentially spherical and have an average diameter of 105±30 nm. Their zeta-potential was around -25 mV and very close values were found for the nanoparticles prepared using the other two solvents. Such a high negative value of zeta-potential indicates the occurrence of a high concentration of free carboxyl groups on the particle surface.

According to the blocky microstructure of the *co*PMLA-(Me$_{75}$H$_{25}$) chain, the structure of these nanoparticles can be interpreted as if the short sequences of malic acid units were segregated to the outer part of the nanospheres whereas the longer homogeneous methyl malate segments were preferably located in the particle core. The surface location of the carboxyl groups will facilitate their chemical modification as well as their ionic coupling with cationic species.

Furthermore, a high zeta potential value is a favorable feature for nanoparticle stability because aggregation will be hindered by electrostatic repulsion. In fact, the size distribution profile displayed by *co*PMLA-(Me$_{75}$H$_{25}$) nanoparticles prepared in DMSO was essentially retained after freeze-drying (Figure 1b).

8.3.2. Hydrolytic degradation. The hydrolytic degradation of *co*PMLA-(Me$_{75}$H$_{25}$) disks has been recently reported.[15] It was there shown that the molecular weight of the copolymer decreased to a fifth of its initial value in a period of 10 days when incubated at 37 ºC and pH 7.4. Degradation took place by hydrolysis of the methyl carboxylate side groups followed by hydrolysis of the main chain ester groups. *co*PMLA-(Me$_{75}$H$_{25}$) nanoparticles displayed almost the same behavior.

As it can be seen in Figure 2, the weight-average molecular weight of the copolymer fell down from 35,000 to about 5,000 after 12 days of incubation PBS under physiological conditions.
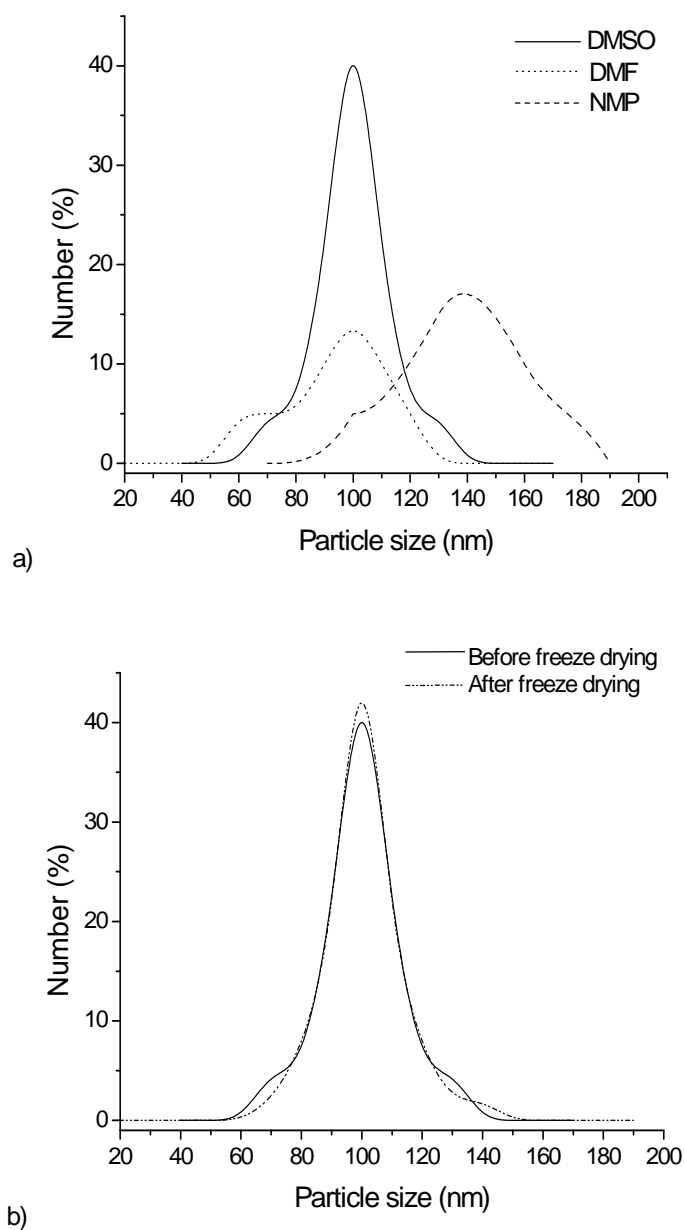
Figure 1. a) Particle size distribution of *co*PMLA-(Me$_{75}$H$_{25}$) nanoparticles prepared using the indicated solvents. b) Effect of freeze-drying on the size of nanoparticles obtained using DMSO as solvent.

A similar reduction in molecular size but taking place at significantly higher rates was observed upon incubation at both pH 4.0 and pH 11. Addition of lipase increased even more the hydrolysis rate evidencing the sensitivity of *co*PMLA-(Me$_{75}$H$_{25}$) to enzymatic activity.
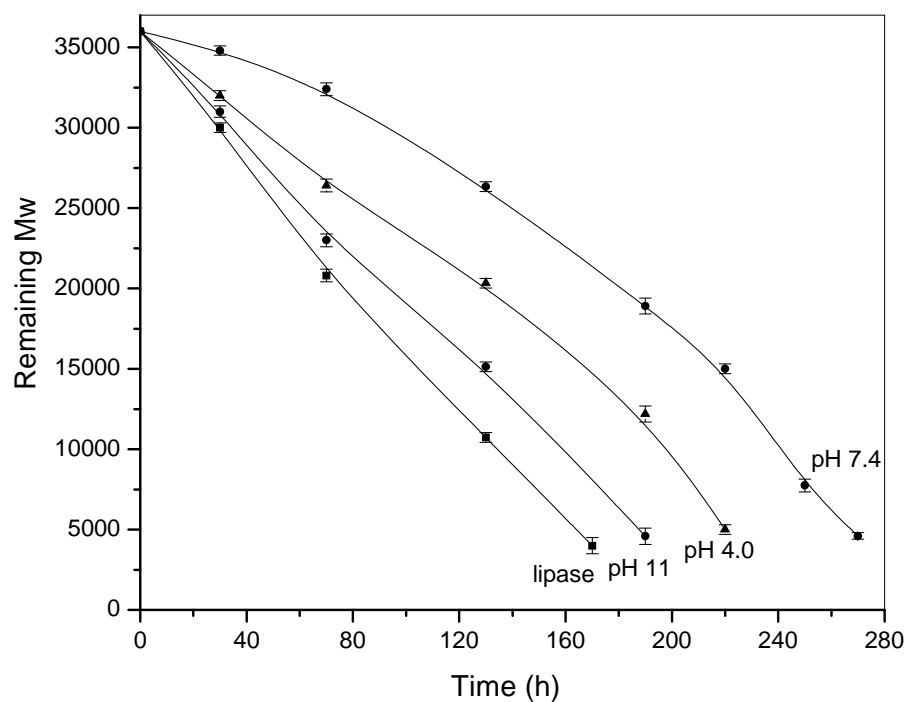
Figure 2. Effect of pH and enzyme (lipase) in the hydrolytic degradation of *co*PMLA-(Me$_{75}$H$_{25}$) nanoparticles at 37 ºC.
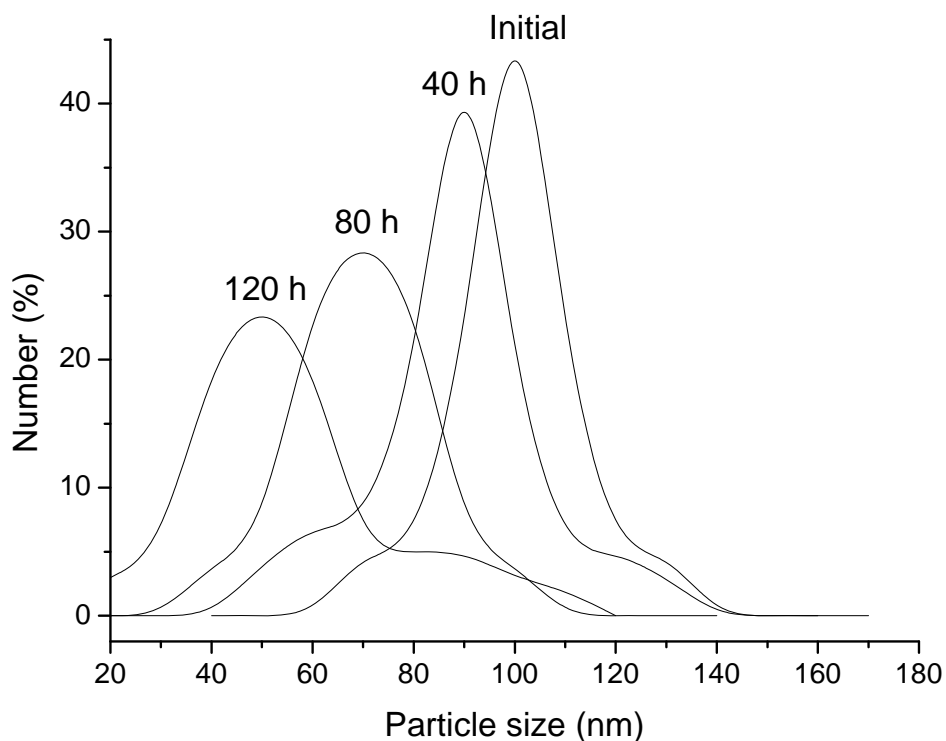
Figure 3. Changes in the particle size of *co*PMLA-(Me$_{75}$H$_{25}$) nanoparticles as a function of degradation time at pH 7.4 and 37 ºC.

The dimensional and morphological changes taking place in the nanoparticles upon degradation at pH 7.4 and 37 ºC were followed by NIBS and SEM. As shown in Figure 3, the particle size was found to decrease gradually so that their mean diameter became less than half of the initial value after 120 h of incubation whereas dispersity did not appear to broaden significantly.
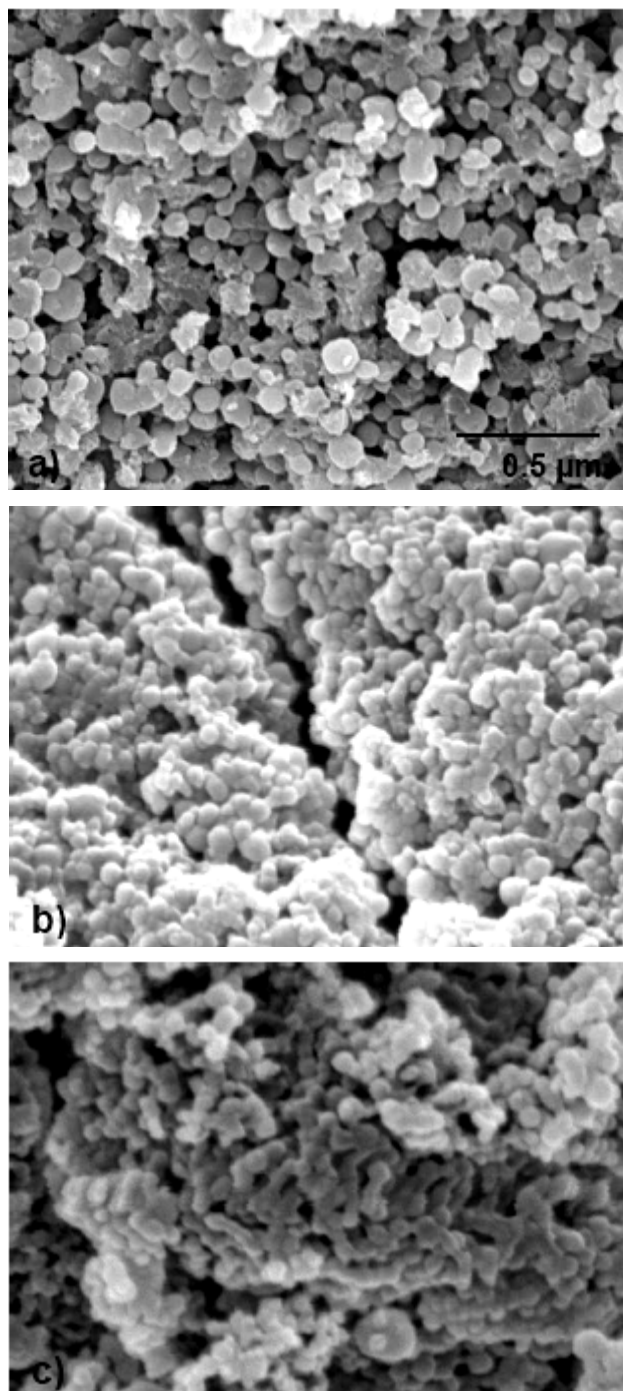
Figure 4. SEM images of coPMLA-(Me$_{75}$H$_{25}$) nanoparticles subjected to hydrolytic degradation. a) initial sample, b) after 80 h of degradation and c) after 200 h of degradation.

In the SEM pictures of Figure 4, the appearance of the nanoparticles before and after degradation for periods of 80 and 200 h are compared. The initially well defined spherical particles were deformed and reduced in size to finally collapse in an almost continuous mass where the particle shape could be hardly discerned.

These results suggest that degradation of nanoparticles must occur preferentially on the surface of the particle with subsequent solubilization of the fragmented chains. This mechanism would be supported by the fact that the reduction observed in particle size is clearly higher than expected from the changes measured in molecular weight distribution.

8.3.3. Entrapment of protein into the nanoparticles. In order to evaluate the capacity of these nanoparticles as a protein carrier system, six proteins differing in molecular weight and/or isolectric point were used in loading essays applying three different loading methods, encapsulation, physical absorption and chemical immobilization. The main features of these proteins and resulting loaded nanoparticles are compared in Table 2 and 3.

Table 2. Protein features.

Nanoparticles	Mw (kDa)	Isolectric point
Unloaded	-	-
Loaded		
BSA	69.0	4.9
β-Lactoglobulin	18.0	5.2
Myoglobin	17.5	7.3
α-Chymotrypsin	25.0	9.1
Cytochrome	12.5	10.2
Lysozyme	14.5	11.0

Table 3. Nanoparticle features.

	Zeta potencial (mV) Method[a]			Particle size ± SD (nm) Method[a]		
Nanoparticles	I	II	III	I	II	III
Unloaded		-25.2 ± 1.1			105 ± 31	
Loaded						
BSA	-21.5 ± 2.1	-26.3 ± 2.3	-29.5 ± 2.1	180 ± 36	110 ± 22	120 ± 34
β-Lactoglobulin	-23.2 ± 2.2	-27.2 ± 2.2	-28.1 ± 2.3	120 ± 27	119 ± 20	110 ± 27
Myoglobin	-25.1 ± 2.5	-25.1 ± 2.1	-25.6 ± 2.2	133 ± 23	120 ± 26	128 ± 22
α-Chymotrypsin	-19.8 ± 2.0	-17.8 ± 2.5	-18.4 ± 2.4	146 ± 31	128 ± 28	133 ± 25
Cytochrome	-18.5 ± 2.3	-16.7 ± 2.1	-16.8 ± 2.1	162 ± 34	133 ± 34	150 ± 35
Lysozyme	-17.4 ± 1.7	-14.5 ± 1.9	-13.8 ± 2.4	170 ± 39	142 ± 35	152 ± 31

[a]Method I: Encapsulation; Method II: Physical absorption; Method III: Chemical immobilization.

Protein encapsulation was performed by coprecipitation upon mixing the aqueous solution of the selected protein and the DMSO solution of coPMLA-(Me$_{75}$H$_{25}$). The absorbed nanoparticles were prepared by simply placing them in contact with the protein aqueous solution. Results obtained in these essays are comparatively plotted in Figure 5.
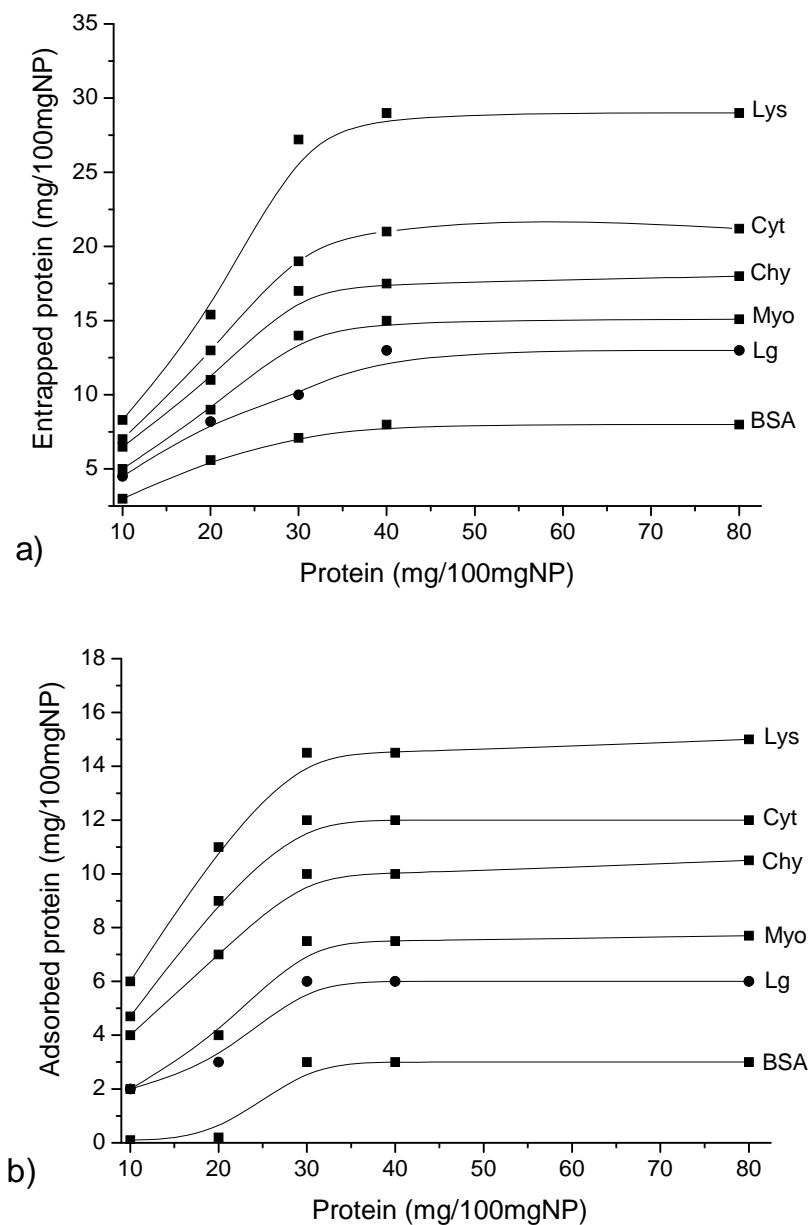
Figure 5. Effect of the protein concentration on the amount of protein encapsulated (a) and adsorbed (b) in coPMLA-(Me$_{75}$H$_{25}$) nanoparticles.

In both cases and for all the proteins essayed, the amount of entrapped protein increased with the used protein/nanoparticle ratio up to reach saturation for an approximate ratio of 0.3-0.4 (w/w).

On the other hand, the loading efficiency was observed to be highly depending on both the protein nature and the applied entrapping method. Thus, the maximum amount of encapsulated protein ranged from 5% for the rather acidic BSA up to near 30 % for the fairly basic lysozyme. This range shifted down to 3-15 % when proteins were physically absorbed.

The potential zeta was modified upon loading in an extension and sign that depended mainly on the protein isolectric point, the changes being more perceivable for absorbed-protein nanoparticles. In both cases, the size of the particles increased in parallel to the amount of entrapped protein but without apparent change in size distribution. The increment in size was more noticeable in the case of protein-encapsulated nanoparticles, the diameter becoming almost doubled for the BSA and Lys loaded particles.

As it was revealed by SEM for the case of myoglobine-encapsulated nanoparticles (Figure 6), neither morphological alterations nor aggregation of the particles took place upon loading. This behavior contrasts to that reported for other amphyphilic nanosystems[18] in which the particle diameter became multiplied by three and size dispersity increased dramatically upon protein loading due to swelling and electrostatic repulsion effects.

In the present case it is assumed that the particle size increment results mainly from mass addition whereas the contribution of other expansive effects may be neglected.

A somewhat different situation was encountered with nanoparticles bearing chemically immobilized proteins. In these nanoparticles, the surface carboxylic groups were activated with WSC so that proteins become covalently attached by amide linkages.

The dependence of the amount of loaded protein with the concentration of WSC used for coupling is plotted in Figure 7. The trend observed in this plot is similar to that observed for the other entrapping methods with loading efficiencies being similar to those achieved by the absorption method. The zeta-potential of the protein-immobilized nanoparticles was found to oscillate in a wider range of values without apparent reasoning. On the other hand, the particle size increased less than in the other cases although size dispersity became relatively wider.
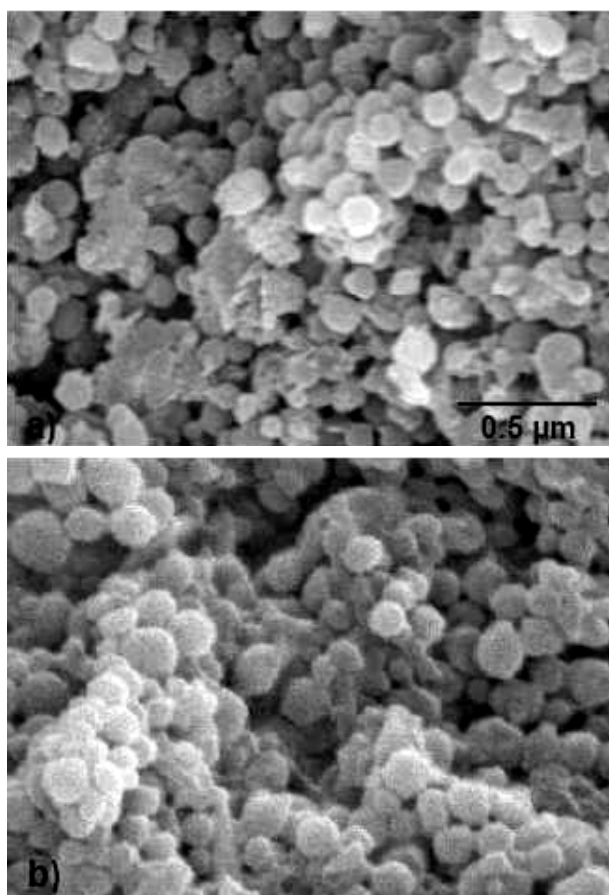
Figure 6. SEM images of nanoparticles of coPMLA-(Me$_{75}$H$_{25}$) illustrating the effect of loading on particle morphology. a) Unloaded particles. b) Myoglobine entrapped nanoparticles.
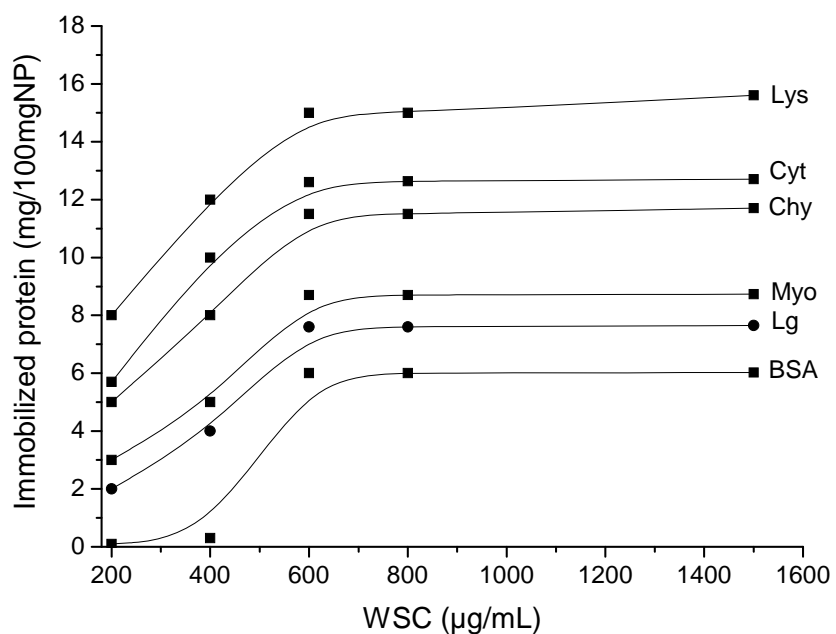
Figure 7. Effect of the concentration of carbodiimide used for coupling on the amount of protein immobilized onto *co*PMLA-(Me$_{75}$H$_{25}$) nanoparticles.

8.3.4. In vitro protein releasing from loaded coPMLA-(Me₇₅H₂₅) nanoparticles. The releasing profiles obtained upon incubation in PBS at pH 7.4 and 37°C for the six proteins studied and the three entrapping methods used in this work are compared in Figure 8.

A common feature to all these plots is that proteins are delivered in periods of times of length similar to that required for the hydrolytic degradation of the nanoparticles suggesting a close connection between the two processes.

A detailed comparison of these profiles led to the following conclusions:

a) Whichever method is used for protein entrapping, the global releasing rate decreased as the isoelectric point of the protein increased evidencing the influence of the protein-polymer ionic interaction on the delivering process.

b) Profiles displayed by both protein-encapsulated and -immobilized nanoparticles (Figures 8a and 8c) are complex and similar in shape. In the two cases, a latency period of 3-4 hours is followed by a more or less steady active period, along which the protein is delivered completely in 6-8 hours. The occurrence of a lag time in the releasing process indicates that polymer has to be degraded in a certain extension for protein being able to leave the nanoparticle.

c) Two groups of protein-absorbed nanoparticles are distinguishable according to their releasing pattern (Figure 8b). The acidic proteins (Ip lower than 7.0) are delivered evenly and fast whereas the basic ones (Ip higher than 7.0) are released following a complex pattern similar to that observed for the nanoparticles loaded by the other two methods. The different behavior observed for the two groups is thought to be due to protein-PMLA ionic interactions.

The strong ionic coupling between the PMLA carboxylic and protein amine groups is resistant to solvolysis so that polymer degradation is required for protein releasing.

As a result, the releasing behavior of basic proteins-absorbed nanoparticles is similar to that displayed by protein-covalently grafted nanoparticles. Since polymer degrades generating malic acid, it is likely that the release of chemically bound proteins yields proteins bearing MLA residues (amide bond being more resistant than ester bonds to hydrolytic degradation). Conversely, acidic proteins are attached by weak interactions and they are rapidly liberated by desorption.

d) A common fact that is observed for all the releasing profiles is that a small amount of protein (less than 10%) is released at the beginning of incubation; this initially released protein is that absorbed on the nanoparticle surface that was not removed by washing. In the case of the acidic protein-absorbed nanoparticles (Figure 8b), the whole loaded protein is weakly attached to the nanoparticle surface and therefore liberated according to such pattern.

8.3.5. Protein activity loss. Protein unfolding is a usual inconvenient affecting to polymeric carrier systems in which specific protein-polymer interactions occur. We have preliminary evaluated the effect of loading and releasing on the activity of proteins entrapped in *co*PMLA-(Me$_{75}$H$_{25}$) by using α-chymotrypsin as a model.

The activity measured for free α-chymotrypsin and α-chymotrypsin released from loaded *co*PMLA-(Me$_{75}$H$_{25}$) nanoparticles as a function of time is plotted in Figure 9 for the three used loading methods. As expected, the enzyme activity decreased with time to practically disappear after ten days of incubation. Nevertheless, significant differences were observed depending on the entrapping method.

Comparison of the specific activity at time zero reveals that encapsulation and physical absorption hardly had detrimental effect on enzyme activity whereas chemical immobilization entailed a 50% of activity loss. On the other hand, a comparison of the plot slopes reveals that the rate of activity loose was lower in the case of the encapsulated protein than in the other cases including free protein.

It can be inferred therefore that encapsulation helps to preserve α-chymotrypsin activity whereas no beneficial effects are noticed when the enzyme was loaded using the other loading methods. It should be stressed that for encapsulation the protein enters in contact with DMSO, which is used for dissolving the polymer. Apparently, this solvent does not alter dramatically the conformation of the protein and the encapsulating polymer contributes to its preservation in the aqueous environment.
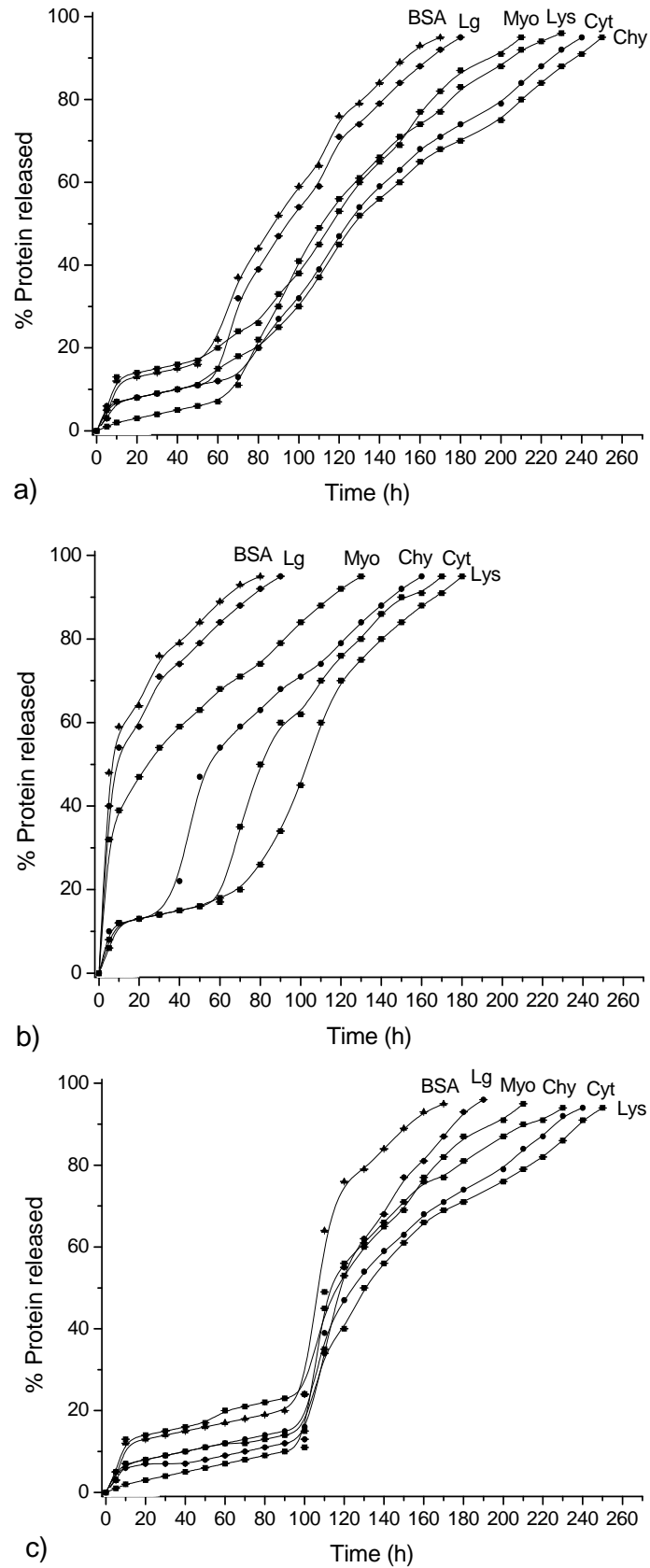
Figure 8. Releasing profiles at pH 7.4 and 37°C of proteins entrapped in coPMLA-(Me$_{75}$H$_{25}$) nanoparticles. a) Encapsulated, b) physically adsorbed, and c) chemically immobilized.
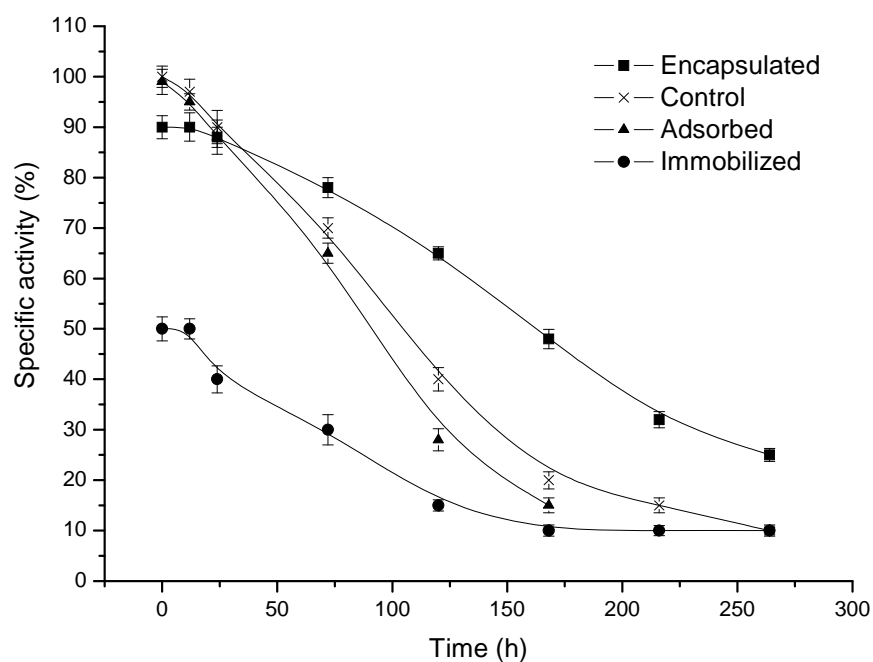
Figure 9. Decrease of the specific activity of α-chymotrypsin as a function of releasing time (values are corrected taking into account the amount of enzyme liberated at each time).

8.4. Conclusions

The fungal PMLA based copolyester *co*PMLA-(Me$_{75}$H$_{25}$) may be used for the manufacture of stable nanoparticles with a diameter in the 100 nm range and a fairly narrow size distribution. These nanoparticles are readily degradable in the aqueous environment at a rate that is depending on pH and the presence of lipase. Proteins can be loaded in these nanoparticles with an efficiency that is determined by the nature of the protein and the method used for entrapping.

Upon incubation under physiological conditions, encapsulated and chemically immobilized proteins are released encompassing polymer degradation. A preliminary study indicates that encapsulation in *co*PMLA-(Me$_{75}$H$_{25}$) nanoparticles delays the activity loss of α-chymotrypsin. It can be concluded from the results obtained in this work that *co*PMLA-(Me$_{75}$H$_{25}$) nanoparticles constitute an interesting protein carrier system with potential in biopharmaceutical applications for the delivery of proteins and peptides.

8.5. References

1. L. Brannon-Peppas, J.O. *Adv. Drug Deliv. Rev.* **2005**, *56*, 1649.
2. K.S. Soppimath, T.M. Aminabhavi, A.R. Kulkarni, W.E. Rudzinski, *J. Control. Rel.* **2001**, *70*, 1.
3. J. Panyam, V. Labhasetwar, *Adv. Drug Deliv. Rev.* **2003**, *55*, 329.
4. S. Cohen, T. Yoshioka, M. Lucarelli, L.H. Hwang, R. Langer. *Pharm. Res.* **1991**, *8*, 713.
5. J. Panyam, M.M. Dali, S.K. Sahoo, W. Ma, S.S. Chakravarthi, G.L. Amidon, R.J. Levy, V. Labhasetwar, *J. Control. Release* **2003**, *92*, 173.
6. I.J. Castellanos, G. Cruz, R. Crespo, K. Griebenow, *J. Control. Release* **2002,** *81,* 307.
7. I.J. Castellanos, R. Crespo, K. Griebenow, *J. Control. Release* **2003**, *88*,135.
8. B.S. Lee, M. Vert, E. Holler, Water-soluble aliphatic polyesters: Poly(malic acid)s. In: Y. Doi, A. Steinbüechel (Eds.) Biopolymers, vol. 3, Wiley-VCH, Weinheim, 2002.
9. D. Domurado, P. Fournié, C. Braud, M. Vert, P. Guérin, F. Simonnet, *J. Bioact. Compat. Polym.* **2003**, *18*, 23.
10. S. Cammas, M-M. Béar, L. Moine, R. Escalup, G. Ponchel, K. Kataoka, Ph. Guérin, *Int. J. Biol. Macromol.* **1999**, *25*, 273.
11. M. Fujita, N.M. Khazenzon, A.V. Ljubimov, B.S. Lee, I. Virtanen, E. Holler, K.L. Black, J.Y. Ljubimova, *Angiogenesis* 2006, *9*, 183.
12. B.S. Lee, M. Fujita, N.M. Khazenon, K.A. Wawrowsky, S. Wachsmann-Hogiu, D.l. Farkas, K.L. Black, J.Y. Ljubimova and E. Holler, *Bioconjug. Chem.* **2006**, *17*, 317.
13. J.A. Portilla-Arias, M. García-Alvarez, A. Martínez de Ilarduya, E. Holler, S. Muñoz-Guerra, *Biomacromolecules* **2006**, *7*, 161.
14. J.A. Portilla-Arias, M. García-Alvarez, A. Martínez de Ilarduya, S. Muñoz-Guerra, *Macromol. Biosci.* **2007**, *7*, 897.
15. J.A. Portilla-Arias, M. García-Alvarez, A. Martínez de Ilarduya, E. Holler, J.A. Galbis, S. Muñoz-Guerra, *Macromol. Biosci.* **2008** *(In press)*
16. E. Holler. In: N.P. Cheremisinoff (Ed.), Handbook of Engineering Polymeric Materials, 93-103, Marcel Dekker, New York, 1997.
17. G.L. Peterson, *Anal. Biochem.* **1977**, *83*, 346.
18. T. Akagi, T. Kaneko, T. Kida, M. Akashi, *J Control. Release* **2005**, *108* 226.